

Antiferromagnet topological insulators with AB_2C Heusler structure

C. Li, J. S. Lian, and Q. Jiang*

Key Laboratory of Automobile Materials (Jilin University), Ministry of Education, and School of Materials Science and Engineering, Jilin University, Changchun 130022, China

(Received 12 March 2011; published 13 June 2011)

The band structures, partial density of states, and electronic configuration of several AB_2C full-Heusler compounds have been simulated using local-density approximation (LDA) + U . Results show that full-Heusler compounds with half-filled d orbitals and $d^5d^5s^2p^6$ electronic structures can also form topological insulators, which will double the range of topological insulator candidates. The band structures of full-Heusler compounds are affected by the covalent bondings of $A-B$ and $B-C$ jointly. The spin-up electrons and spin-down electrons influence the orbitals respectively, which leads to the magnetism of the materials, and all full-Heusler compounds with the magnetic moments $\sim 9\mu_B$ are antiferromagnets, which may provide a new design of a tunable optical modulator.

DOI: 10.1103/PhysRevB.83.235125

PACS number(s): 73.20.At, 73.43.-f, 73.61.Le, 75.50.-y

I. INTRODUCTION

Topological insulators (TIs) with a full insulating gap in the bulk, but with topologically protected gapless states on their edges or surfaces, are a relatively new class of quantum matter which has attracted great attention theoretically and experimentally.¹⁻³ These electronic materials with strong spin-orbit coupling and band inversion at Fermi level E_F are predicted to exhibit a host of unusual phenomena associated with their nontrivial surface states, such as the image monopole effect,⁴ axions,⁵ and Majorana fermions.⁶ Moreover, the strong TIs are mostly used for quantum wells and have possible applications in new spintronic devices.^{7,8}

TIs have been expanded from two-dimensional materials (HgTe¹) to three-dimensional ones [Bi_{1-x}Sb_x alloys,⁸ Bi₂Sb₃, Bi₂Te₃, Sb₂Te₃,^{9,10} half-Heusler compounds (HHCs),¹¹⁻¹³ pyrochlores,^{14,15} Kondo insulators,¹⁶ and thallium-based ternary chalcogenides.¹⁷ Vigorous searches for the new topologically nontrivial phases are needed to enlarge the number of candidate crystalline structures and find various properties such as magnetism, superconductivity, or heavy fermion behavior, because a number of spectacular quantum phenomena have been predicted when the surface states are affected by magnetism and superconductivity.^{11,12,17} Up to now, most known TI candidates are nonmagnetic, except for several ferromagnetic LnPtBi and LnPtSb (Ln = lanthanide) compounds where rare-earth elements with strongly correlated f electrons can exhibit better magnetism; the magnetic moments have varied from zero in La up to $>10\mu_B$ in Dy or Ho, leading to strong magnetic ground states harbored in the LnPtBi or LnPtSb series.¹¹ The lanthanide series, however, have different numbers of spin up (n_\uparrow) and spin down (n_\downarrow) and induce the separating band structures of spin up and spin down near the E_F [see Fig. 1(a)]. Thus, these materials are metallic; despite this they can transition into TIs by a single axis stress.¹¹ In order to gain convenient magnetic application in the quantum-spin Hall state, more magnetic TI candidates need to be prepared.

For the demand of magnetic TIs, we have considered the AB_2C full-Heusler compounds (FHCs) with MnCu₂Al-type $L2_1$ structure where A and B are transition or rare-earth metals and C denotes the main-group elements, as many FHCs are magnetic^{18,19} and the inversion symmetry characteristic

of FHCs is propitious to form TIs.¹ Moreover, comparing FHCs with the known TI HHCs, their crystal structures are similar; the structure of AB_2C HHCs (AB_2C FHCs) can be considered as being composed of three (four) interpenetrating face-centered-cubic lattices with positions described with the Wyckoff coordinates where atoms are arranged at the positions A (1/2, 1/2, 1/2), B' (1/4, 1/4, 1/4) [B (1/4, 1/4, 1/4), and (3/4, 3/4, 3/4)] and C (0, 0, 0). To obtain the topological state materials, the FHCs should have an electronic structure similar to the known TIs with HHC structure. Taking into account that HHCs have 18 valence electrons with a closed atomic K shell ($d^{10}s^2p^6$),¹¹ the selected FHCs thus also have 18 valence electrons, keeping valance electrons of $A + C = 8$, and two B atoms with five valence electrons of each atom replace one B' atom, and FHCs with ($d^5d^5s^2p^6$) electronic structures compare with HHCs with ($d^{10}s^2p^6$). Although the d orbital is half filled in FHCs, their electronic structures may satisfy this criterion also and AB_2C (when A and C are properly selected) thus may be a TI.

In this paper, by using the first-principles simulation, we predict a potentially new class of magnetic TIs of AB_2C FHCs. The valance electrons of $A + C$ are always selected to be eight; namely, they are IV + IV or IIIB + V elements. B elements must be VB elements with five valence electrons. Corresponding band structures, partial density of states (PDOS), and electronic configuration have been carried out to support the prediction. The mechanism of the magnetism of FHCs is also discussed.

II. METHODS

Band structures, PDOS, and electronic configuration of several AB_2C FHCs were determined based on the density functional theory (DFT) with Perdew-Burke-Ernzerhof (PBE) functional of generalized gradient approximation (GGA) and with ultrasoft pseudopotentials,²⁰ as implemented in the CASTEP code.²¹ Geometry optimizations of all structures are made on conventional unit cells using ultrafine cutoff energies for the plane-wave expansion. The k -point sampling set is a $10 \times 10 \times 10$ division of the reciprocal unit cell based on the Monkhorst-Pack scheme.²² The convergence

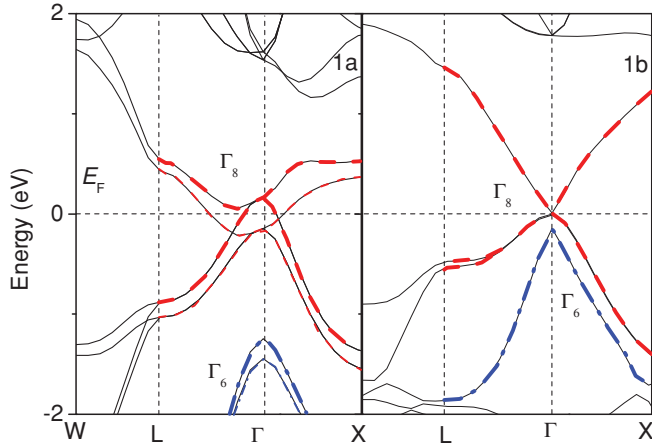


FIG. 1. (Color online) Band structures of GdPtBi (1a) and YV₂Bi (1b), where the dotted line marks the bands with Γ_6 symmetry and the dash-dotted line is that of Γ_8 symmetry. The heavy line marks spin up and thin line is spin down.

tolerance of energy of 5.0×10^{-6} eV/atom, maximum force of 0.01 eV/Å, and maximum displacement of 5.0×10^{-4} Å were used. Spin polarized and local-density approximation (LDA)+ U ²³ have been used because LDA + U is now a well-established model to deal with electron correlations in transition metal and rare-earth compounds, which guarantees the electronic structures of these materials being consistent with that of experimental results.²⁴ In the LDA + U method, the strong correlation between localized d electrons is explicitly taken into account through the screened effective electron-electron interaction parameter U .

III. RESULTS AND DISCUSSION

Figure 1 shows a comparison of band structures between GdPtBi [Fig. 1(a)] and YV₂Bi [Fig. 1(b)]. They both are inverted bands with Γ_6 (twofold symmetry) (dotted line) lying below the Γ_8 (fourfold symmetry) (dash-dotted line). This is the necessary condition for TI state because it changes the parity of the wave function compared with semiconductors such as HgTe.¹¹ The band structures of n_\uparrow (thick line) and n_\downarrow (thin line) are separated in GdPtBi, being ferromagnetic and metallic; while in YV₂Bi, the band structures of spin up and spin down are uniform without a gap. Although the metallic GdPtBi can be transitioned into the TI state by a single axial stress,¹¹ YV₂Bi without a gap is more suitable for TIs. Moreover, YV₂Bi with a zero gap and inverted bands has proved that the half-filled d orbitals can also form TIs, which will obviously enlarge the boundaries of searching for new TI candidates.

Figure 2 shows the PDOS of YV₂Bi, where positive values along the y axis denote n_\uparrow and negative values n_\downarrow . It is obvious that n_\uparrow and n_\downarrow of the Y or Bi atom are the same, while that of V atoms are different: $n_\uparrow n_\downarrow$ for V1 atom and $n_\uparrow < n_\downarrow$ for V2 atom, where V1 and V2 denote atoms in a primitive cell at different locations. Although the total numbers of n_\uparrow and n_\downarrow in a primitive cell are the same, V1 atom has a magnetic moment of $2.52\mu_B$ and V2 atom has that of $-2.52\mu_B$. In total, YV₂Bi is an antiferromagnet with the magnetic moment of

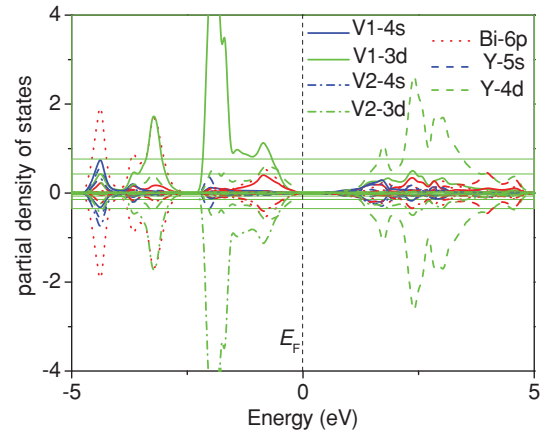


FIG. 2. (Color online) The PDOS of YV₂Bi, where positive values on the y axis denote spin up and negative ones denote spin down.

$9.21\mu_B$ calculated by our simulation. The conduction band minimum consists mostly of Y-4*d*, Y-5*s*, V-4*s*, and Bi-6*s* orbitals; the valence band maximum is composed of V-3*d*, V-4*s*, Bi-6*p*, and Y-4*d* electrons. Some V-3*d*, V-4*s*, Bi-6*p*, and Y-5*s* electrons hybridize together and form a new bonding orbital between -4.8 and -2.6 eV. Moreover, the capability of d orbitals near E_F of each V atom is five. Thus, the rest of the d orbitals should have higher energy and be away from E_F , which implies that half-filled d orbitals here have a function similar to a filled d orbital and are also suitable for TIs. All considered FHCs listed in Table I have similar results with the magnetic moments $\sim 9\mu_B$. This is the spin-wave excitation coupled topologically with an electromagnetic field, which as bulk magnetism may realize the dynamical axions. Such an effect provides a potentially new design for tunable optical modulators.⁵

TABLE I. Magnetic moments with units μ_B of the materials. e_x , e_y , and e_z are the Mulliken charge of X, Y, and Z elements, respectively.

Compounds	Magnetic moment	e_x	e_y	e_z
ScV ₂ P	9.39	0.25	-0.02	-0.21
ScV ₂ Sb	9.00	0.39	0.02	-0.43
ScV ₂ As	9.43	0.35	0.07	-0.49
ScV ₂ Bi	9.50	0.18	-0.06	-0.07
YV ₂ P	8.62	1.29	-0.26	-0.77
YV ₂ Sb	9.09	1.16	-0.50	-0.16
YV ₂ As	8.82	0.99	-0.30	-0.39
YV ₂ Bi	9.21	0.95	-0.40	-0.15
LaNb ₂ P	7.79	0.52	-0.20	-0.12
LaNb ₂ Sb	7.29	1.00	-0.29	-0.42
LaNb ₂ As	7.99	0.73	-0.18	-0.37
LaNb ₂ Bi	7.45	0.91	-0.31	-0.29
HfNb ₂ Si	7.43	0.95	-0.19	-1.57
HfNb ₂ Sn	8.00	0.94	-0.43	-0.08
HfNb ₂ Pb	8.15	0.92	-0.23	-0.46
GdPtBi	7.35	1.02	-1.03	0.01
DyPtBi	10.3	0.74	-0.80	0.06

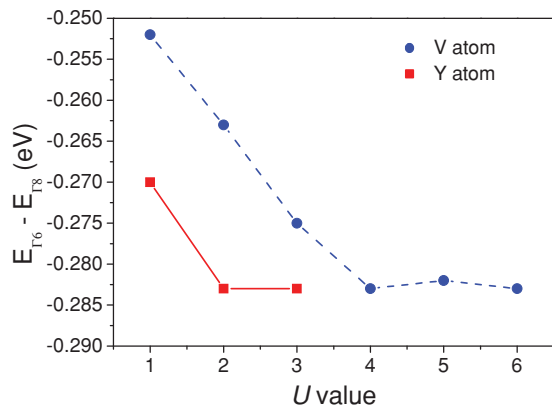


FIG. 3. (Color online) The energy difference between Γ_6 and Γ_8 bands ($E_{\Gamma_6}-E_{\Gamma_8}$) of YV_2Bi as a function of different U values of Y and V atoms.

To compare influences of different U values on the electronic structure, we calculate all considered materials with different U values. Taking YV_2Bi as an example, we change the U values of Y and V atoms. The results of corresponding band structures calculated for $E_{\Gamma_6}-E_{\Gamma_8}$ are shown in Fig. 3, where \bullet and \blacksquare denote V and Y atoms, respectively. It is found that the values of $E_{\Gamma_6}-E_{\Gamma_8}$ decrease as the U values of V atoms decrease from 1 to 4 eV. When $U=4, 5$, or 6 eV, the values of $E_{\Gamma_6}-E_{\Gamma_8}$ change little. Thus, $U=4$ eV for the V atom could be adequate to deal with electron correlations. Similar calculations are carried out for the Y atom, and $U=2$ eV is obtained. Note that when $U=0$, YV_2Bi becomes a conductor, which implies that the LDA + U technique is necessary for the simulation in our case. At the same time, changes of U values of Y and V atoms hardly change the total magnetic moments of YV_2Bi (see Table II). All considered materials have the same results as previously mentioned. Thus, $U=2$ eV for Sc, Y, and La, $U=3$ eV for Hf, $U=4$ eV for V and Nb, were taken respectively.

To analyze the detailed bonding of each atom, we show the electronic configuration of YV_2Bi in Fig. 4. It is generally found that the electron distributions of higher and lower energy levels are quite different. We considered the spin-up electrons first; when orbitals are at -4.8 to -2.6 eV, almost all electrons are fixed between Bi and the V (denoted as V1) atoms on the left-hand side, which definitely proves the existence of strong covalent bonds with sdp^2 hybridization forming by $V-3d$, $V-4s$, and $Bi-6p$ electrons where the V1 atom has fourfold covalent bonds with four Bi atoms. While comparing with the PDOS, a few $Y-5s$ and $Y-4d$ electrons should be limited around the Y atom and have little effect with the V or Bi atom. For orbitals at -2.2 to -1.7 eV, similarly, these are strong

TABLE II. Magnetic moments of YV_2Bi with different U values of Y and V atoms with units μ_B .

V Y	U = 1	U = 2	U = 3	U = 4	U = 5	U = 6
U = 1				9.20		
U = 2	8.35	8.72	9.01	9.21	9.42	9.58
U = 3				9.22		

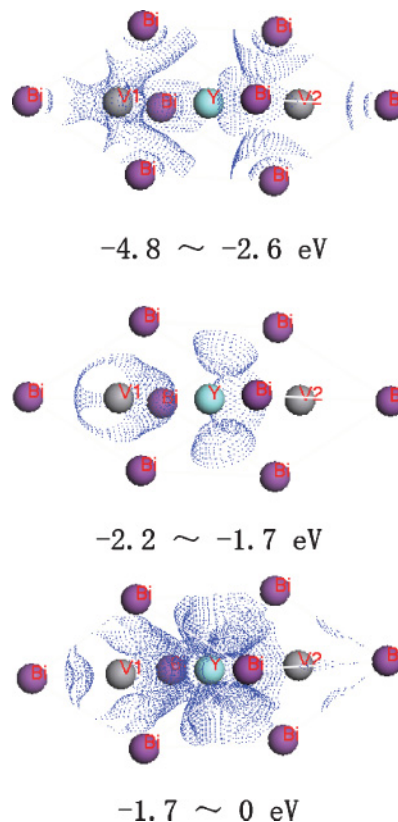


FIG. 4. (Color online) The spin-up orbital of electronic configuration of YV_2Bi at different energy levels.

covalent bonds forming by $V-3d$, $Y-5s$, and $Y-4d$ electrons where the Y atom has fourfold covalent bonds with four V1 atoms. While for orbitals at $-1.7-0$ eV (E_F is set at 0 eV), there are two kinds of covalent bonds: $Y-V$ and $V-Bi$; the $Y-V$ bonding is obviously stronger than $V-Bi$ bonding, which is reasonable as the difference of Pauling electronegativities between Y and V elements ($\chi_V-\chi_Y$) is smaller than ($\chi_{Bi}-\chi_V$), where the subscripts denote corresponding elements and $\chi_Y=1.22$, $\chi_V=1.63$, and $\chi_{Bi}=2.02$.²⁵ On the other hand, when the spin-down electrons have been considered, the orbital distributions of spin-down electrons are similar to those of spin-up electrons; the orbitals are just around the right-hand V (denoted as V2) atom, not V1. Y and Bi atoms in any case have little effect. Combining the results of Figs. 2 and 4, the covalent bonds of $Y-V$ and $V-Bi$ jointly influence the band structures of YV_2Bi . The spin-up electrons and spin-down electrons affect the orbitals respectively and induce the magnetism, which is different from HHCs.¹²

To illustrate the impressive number of potentially new topological compounds and the possibility to tune the $\Gamma_6-\Gamma_8$ bond ordering in this class of materials, we have calculated all relevant FHCs containing Sc, Y, La, and Hf. The energy differences between Γ_6 and Γ_8 bands as a function of the lattice constant of the compounds are shown in Fig. 5. $HgTe$ and $CdTe$ binary compounds are also present for comparison purposes. The compounds with $E_{\Gamma_6}-E_{\Gamma_8}=0$ are insulators, whereas those with $E_{\Gamma_6}-E_{\Gamma_8}<0$ are TI candidates. The latter group consists of zero-gap semiconductors with a doubly degenerated Γ_8 point at E_F . All existing HHCs without gap at E_F under certain

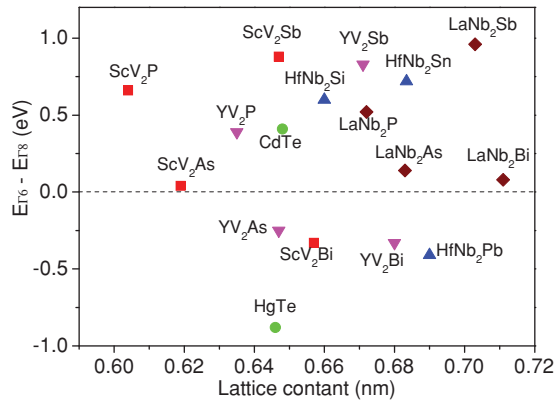


FIG. 5. (Color online) The energy difference between Γ_6 and Γ_8 bands ($E_{\Gamma_6} - E_{\Gamma_8}$) as a function of the lattice constant.

conditions will reveal the same type of band inversion as HgTe does. Pairs of materials with well-matching lattices for the quantum wells can be easily picked up along the same vertical line, such as $\text{ScV}_2\text{Sb}-\text{YV}_2\text{As}$ and $\text{HfNb}_2\text{Sn}-\text{YV}_2\text{Bi}$, similar to $\text{CdTe}-\text{HgTe}$. The borderline ($E_{\Gamma_6} = E_{\Gamma_8}$) compounds, such as ScV_2As , LaNb_2As , and LaNb_2Bi , are situated closer to the zero horizontal line, which can be easily transformed from a common to a topological insulator and vice versa by a small variation of the lattice constant (by applying pressure or growing films on appropriate substrates).¹¹ Combining with sufficiently strong spin-orbit coupling, it leads to a pronounced Γ_6 - Γ_8 band inversion, which is the key to realizing the TI state. The Mulliken charges of all elements of considered insulators are listed in Table I. It is obvious that all X elements are positively charged, while Y and Z elements have mostly negative charges. Most Mulliken charges are <1 . Hence, there is indeed covalent bonding in the compounds which is propitious to form TIs. As a result, the χ difference among distinct elements in our case should be small.

It is known that Heusler compounds with 18 or 24 valence electrons are electron compounds. Our considered compounds

have indeed 18 valence electrons. To further consider the structural stabilities of our used systems, the formation energies of these compounds E_f are determined. $E_f = -5.33$ eV/atom for YV_2Bi , $E_f = -4.63$ eV/atom for YV_2As , $E_f = -4.71$ eV/atom for ScV_2Bi , and $E_f = -4.91$ eV/atom for HfNb_2Pb , which are comparable with existing Heusler compounds of DyPtBi with $E_f = -7.40$ eV/atom, SmPtBi with $E_f = -9.72$ eV/atom, NdPtBi with $E_f = -6.84$ eV/atom, and TbPtBi with $E_f = -9.94$ eV/atom. These data confirm that our considered compounds are thermodynamically at least as stable as the presently known Heusler compounds.

IV. CONCLUSIONS

In summary, band structures, PDOS, and electronic configuration of several AB_2C FHCs have been simulated using $\text{LDA} + U$. The results show that FHCs with half-filled d orbitals and $d^5d^5s^2p^6$ electronic structures can also form TIs, which will double the range of TI candidates. The band structures of FHCs are affected by the covalent bonding of $A-B$ and $B-C$ jointly. The spin-up and spin-down electrons influence the orbitals respectively, which induce the magnetism of the materials. All FHCs with the magnetic moments $\sim 9\mu_B$ are antiferromagnets, which may provide a new design of a tunable optical modulator.

ACKNOWLEDGMENTS

The authors acknowledge the financial support from NNSFC (Grant No. 50571040), National Key Basic Research and Development Program (Grant No. 2010CB631001), Program for Changjiang Scholars and Innovative Research Team in University, and the High Performance Computing Center (HPCC) of Jilin University for supercomputer time.

*jiangq@jlu.edu.cn

¹B. A. Bernevig, T. L. Hughes, and S. C. Zhang, *Science* **314**, 1757 (2006).

²M. König, S. Wiedmann, C. Brune, A. Roth, H. Buhmann, L. Molenkamp, X.-L. Qi, and S.-C. Zhang, *Science* **318**, 766 (2007).

³R. Roy, *Phys. Rev. B* **79**, 195322 (2009).

⁴X.-L. Qi, R. Li, J. Zhang, and S.-C. Zhang, *Science* **323**, 1184 (2009).

⁵R. Li, J. Wang, X.-L. Qi, and S.-C. Zhang, *Nat. Phys.* **6**, 284 (2010).

⁶L. Fu and C. L. Kane, *Phys. Rev. Lett.* **100**, 096407 (2008).

⁷L. Fu, C. L. Kane, and E. J. Mele, *Phys. Rev. Lett.* **98**, 106803 (2007).

⁸D. Hsieh, D. Qian, L. Wray, Y. Xia, Y. S. Hor, R. J. Cava, and M. Z. Hasan, *Nature* **452**, 970 (2008).

⁹Y. Xia, D. Qian, D. Hsieh, L. Wray, A. Pal, H. Lin, A. Bansil, D. Grauer, Y. S. Hor, R. J. Cava, and M. Z. Hasan, *Nat. Phys.* **5**, 398 (2009).

¹⁰Y. L. Chen, J. G. Analytis, J.-H. Chu, Z. K. Liu, S.-K. Mo, X. L. Qi, H. J. Zhang, D. H. Lu, X. Dai, Z. Fang, S. C. Zhang, I. R. Fisher, Z. Hussain, and Z.-X. Shen, *Science* **325**, 178 (2009).

¹¹H. Lin, L. A. Wray, Y. Q. Xia, S. Y. Xu, S. Jia, R. J. Cava, A. Bansil, and M. Z. Hasan, *Nat. Mater.* **9**, 546 (2010).

¹²S. Chadov, X. L. Qi, J. Kübler, G. H. Fecher, C. Felser, and S. C. Zhang, *Nat. Mater.* **9**, 541 (2010).

¹³M. Franz, *Nat. Mater.* **9**, 536 (2010).

¹⁴D. A. Pesin and L. Balents, *Nat. Phys.* **6**, 376 (2010).

¹⁵H.-M. Guo and M. Franz, *Phys. Rev. Lett.* **103**, 206805 (2009).

¹⁶M. Dzero, K. Sun, V. Galitski, and P. Coleman, *Phys. Rev. Lett.* **104**, 106408 (2010).

¹⁷B. Yan, C.-X. Liu, H.-J. Zhang, C.-Y. Yam, X.-L. Qi, T. Frauenheim, and S.-C. Zhang, e-print [arXiv:1003.0074](https://arxiv.org/abs/1003.0074) (2010).

¹⁸J. Li, Y. X. Li, G. X. Zhou, Y. B. Sun, and C. Q. Sun, *Appl. Phys. Lett.* **94**, 242502 (2009).

¹⁹D. C. Dunand and P. Müllner, *Adv. Mater.* **23**, 216 (2011).

²⁰D. R. Hamann, M. Schluter, and C. Chiang, *Phys. Rev. Lett.* **43**, 1494 (1979).

²¹J. P. Perdew, K. Burke, and M. Ernzerhof, *Phys. Rev. Lett.* **77**, 3865 (1996).

²²H. J. Monkhorst and J. D. Pack, *Phys. Rev. B* **13**, 5188 (1976).

²³I. V. Solovyev, P. H. Dederichs, and V. I. Anisimov, *Phys. Rev. B* **50**, 16861 (1994).

²⁴M. Cococcioni and S. Gironcoli, *Phys. Rev. B* **71**, 035105 (2005).

²⁵[<http://www.webelements.com>].